

Review

Vinyl-ruthenium entities as markers for intramolecular electron transfer processes

Philipp Mücke^a, Michael Linseis^a, Stanislav Zálaiš^b, Rainer F. Winter^{a,*}

^a Institut für Anorganische Chemie, Universität Konstanz, Universitätsstraße 10, D-78453 Konstanz, Germany

^b J. Heyrovský Institute of Physical Chemistry, v.v.i, Academy of Sciences of the Czech Republic, Dolejškova 3, 182 23 Prague, Czech Republic

A B S T R A C T

The present account summarizes our work on mononuclear vinyl ruthenium complexes of the type $\text{RuCl}(\text{CH}=\text{CHR}')(\text{CO})(\text{PR}_3)_2\text{L}$, divinyl bridged diruthenium complexes $\{\text{RuCl}(\text{CO})(\text{PR}_3)_2\text{L}\}_2(\mu\text{-CH}=\text{CH}\text{ bridge CH}=\text{CH})$ and on heterobinuclear systems where only one of the two redox active metal organic moieties is of the vinyl ruthenium type. The favourable electrochemical properties of the $\{\text{RuCl}(\text{CO})(\text{PR}_3)_2\text{L}(\text{CH}=\text{CH})\}$ tag and the various spectroscopic handles offered by that unit provide detailed insights into the charge and spin delocalization over the $\{\text{MCl}(\text{CO})(\text{PR}_3)_2\text{L}\}$ and $\text{CH}=\text{CHR}'$ constituents in their associated radical cations. They also offer a convenient means for measuring electronic coupling in the mixed valent radical cations of the homo and heterodinuclear vinyl bridged complexes and, under favourable circumstances, on the rate of intramolecular electron transfer between the individual redox sites. Aspects of this work include examples of complexes showing time dependent valence trapping, complexes aimed at delineating the efficiencies of through space versus through bond pathways for electron delocalization, complexes where electrostatic effects on the redox splitting $\Delta E_{1/2}$ dominate over those from the resonance contribution and systems that exhibit extensive charge and spin delocalization between two dislike endgroups despite their intrinsically different re

Keywords:

Ruthenium

Vinyl complexes

Electrochemistry

Spectroelectrochemistry

Mixed-valent

Contents

1. Introduction	37
2. Mixed valent compounds and experimental measures of delocalization	38
3. The vinyl ruthenium moiety: electron transfer properties and ligand non innocence	41
4. Intramolecular electron transfer in vinyl bridged diruthenium complexes	44
4.1. Linear divinyl bridged diruthenium complexes	44
4.2. Vinyl diruthenium complexes derived from cyclophanes	46
4.3. Mixed systems with only one vinyl ruthenium unit	47
5. Conclusions	49
Acknowledgements	49
References	49

1. Introduction

Establishing and quantifying electronic interactions between interconnected redox active moieties in mixed valent (MV) systems continues to be a matter of considerable interest. Despite the tremendous amount of work devoted to that particular topic, research in this area is still driven by the urge to unravel the mechanisms and pathways by which intramolecular electron transfer in such systems occurs and to measure and control the degree of “electronic communication” between the individual redox sites. This is important from a fundamental and a practical point of view. Electron transfer, i.e. the exchange of an electron or a hole between two redox active molecules or between a molecule and an electrode surface, is one of the two fundamental chemical processes. About 50% of all chemical reactions are believed to involve electron transfer at some point along the reaction path. On the other hand, insight from these studies also flows into the design of molecule based materials for modern electronics [1]. Mixed valent systems are a simple approach to molecular wires, circumventing the need for dealing with the intricacies of connecting individual molecules to electrodes of the macroscopic world and measuring potential/current traces on such delicate arrays. While these issues certainly need to be addressed for any practical application, the fundamental

information as to the intrinsic ability of individual molecules for that use can still be gleaned from such comparatively simple systems.

In this account we present an overview over some of our work on oligonuclear vinyl ruthenium complexes devoted to such issues. Radical cations derived from vinyl bridged diruthenium complexes differ from more “conventional” mixed valent systems in that they show a prevalent contribution of the organic vinyl constituent of these structures to the individual oxidation processes. In the following we will illustrate that these systems form extended metal organic π systems and allow for measuring the charge and spin distribution between (i) the vinyl ligand and the remaining metal coligand moiety on one hand and (ii) between individual vinyl ruthenium/coligand moieties on the other. In doing so, we will first briefly introduce the reader into the topic of mixed valent compounds. Main emphasis will be on the issue of how to obtain experimental information on the strength of the electronic interactions between individual redox active subunits in such systems (the so called “electronic communication”) and on the time scale of intramolecular electron transfer. This will be followed by a brief discussion of the principal properties of vinyl ruthenium complexes and their oxidized forms. Here we will detail why they are so good markers for charge and spin delocalization in extended

multinuclear arrays. We will then present some examples of such systems that we consider as illustrative and instructional. These examples will include linear dinuclear systems as models of electron delocalization in one dimension, cyclophane derived systems as models of three dimensional delocalization through space and unsymmetrical systems with two different redox active moieties, only one of which is of vinyl ruthenium parentage.

2. Mixed-valent compounds and experimental measures of delocalization

Mixed valent (MV) compounds are defined as systems comprising two or more identical (or, in terms of their intrinsic redox potentials, nearly so) redox active moieties in (formally) different oxidation states. In 1969, Creutz and Taube first published their seminal work on the pyrazine bridged bis(pentaammineruthenium)⁵⁺ ion (Chart 1) [2]. This so called Creutz–Taube ion and related systems [3–5] soon gained truly paradigmatic importance for the development of this field. The greater simplicity of these dinuclear systems when compared to sets of separated redox pairs relies on the fact that electron transfer occurs in an intramolecular fashion, thus obliterating separate equilibria like that for the formation of encounter complexes. Moreover, electron transfer is a thermoneutral process with no free energy change once the redox active moieties have identical composition, such that no net thermodynamic driving force needs to be taken into account.

Owing to these circumstances, the Creutz–Taube ion and its immediate relatives with bis(imine) bridging ligands other than pyrazine served as a blueprint for a large host of similar systems that share the same basic construction principle: there are always two (or more) identical or closely related redox active subunits joined by a common “spacer” or “bridge” (Fig. 1; for a stringent definition of these two terms see Ref. [6]). Variations on this general theme come from the choice of the redox active moiety, which may be of inorganic, metal–organic or purely organic nature, and of the bridge, which may be anything from unsaturated and fully

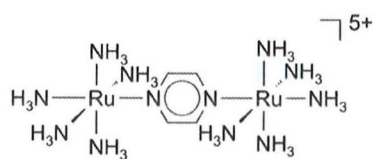


Chart 1. The Creutz–Taube ion.

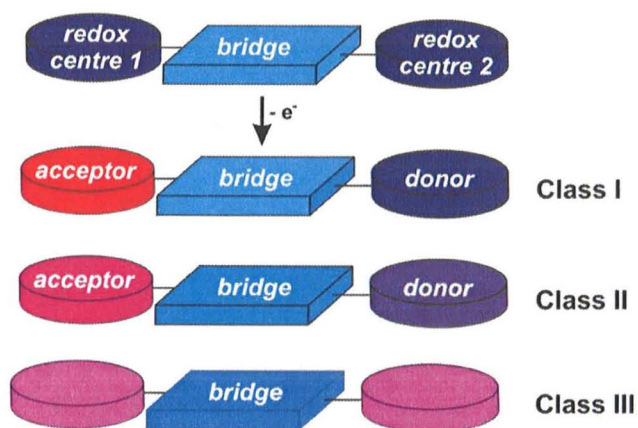


Fig. 1. Schematic representation of the electron distribution in mixed-valent systems of Classes I to III according to Robin and Day.

conjugated to fully saturated. The interaction between the redox active endgroups and the common bridge is another important variable of such systems. Taken together, these alterations allow electronic interactions between the individual redox sites to be modified over several orders of magnitude, thus determining the properties of mixed valent systems in a very profound manner.

This is expressed in the Robin and Day classification scheme [7] where, based on the mutual interactions between the individual redox active subunits, mixed valent (MV) compounds are subdivided into three different classes (Fig. 1). In MV compounds of Class I the bridge essentially behaves as an insulator. This means that the redox active moieties, albeit being of identical composition, differ strongly in their electron densities. Each one shows the same properties as would be observed in a similar system with just one of these moieties in its respective valence state (reduced or oxidized). For systems of Class II, the bridge allows for some degree of electronic interactions between the conjoined local redox sites. This introduces new spectroscopic features that are not present in either isovalent state, most importantly the so called “inter valence charge transfer” (IVCT) band (*vide infra*). In MV compounds of Class II, electronic coupling has the consequence of rendering the redox active termini electronically *more similar* but not to the extent of making them *identical*. There is at least one experimental method which indicates that they are electronically different, i.e. the rate of intramolecular electron transfer is slower than the timescale inherent to that experimental probe of the local electron densities. We will come back to this point in a later section of the present account. MV systems of Class III finally exhibit fully symmetrical charge and spin distributions over both local redox sites. In this scenario the redox sites acquire new (spectroscopic) properties that are connected with their fractional oxidation states that differ from those in the bordering isovalent states. Here it is no longer possible to classify any of the redox sites as a donor or an acceptor. We have tried to symbolize these three different scenarios by the colour coding of Fig. 1 where the individual colours and shades represent the local electron (or spin) densities at the redox sites. More recently, borderline cases of Class II and III MV compounds have been identified as a class of their own [8] with unique properties such as the low energy cutoff of their IVCT band [9,10]. In such systems, the degree of the electronic coupling and “charge equilibration” is particularly sensitive to solvent polarity and the solvation of the individual redox active subunits [11,12].

Like for any other types of reactions, energy changes during intramolecular electron transfer processes can be described by virtue of potential hypersurfaces. Here, the energy is plotted as a function of the so called electron transfer (ET) coordinate (X) in Fig. 2). The typical shapes of such hypersurfaces for MV compounds of Classes I and II are shown as the dotted and solid lines, respectively, in Fig. 2. One might wonder why a degenerate chemical process such as intramolecular ET involves an energy barrier at all. The underlying reason is that ET between redox sites of even identical composition can only occur at a point where the two sites assume identical structures. This pertains to the internal bonding parameters (bond lengths, angles and dihedrals) as well as to the structure of the surrounding solvent shell. Bordering redox states n^+ and $(n+1)^+$, however, usually differ in their intrinsic structures. Here, one only has to think of how ionic radii of metal ions, and, as a consequence, metal–ligand bond lengths change with oxidation state. This means that ET can only occur from a structure that is distorted with respect to the ground state structures of both bordering redox states. The ground state barrier to ET thus reflects the energy required to transform the ground state structures into the distorted, symmetrical one in which ET can occur. In the simplest case the distortion rendering both sites structurally equivalent is brought about by a single fundamental such as a

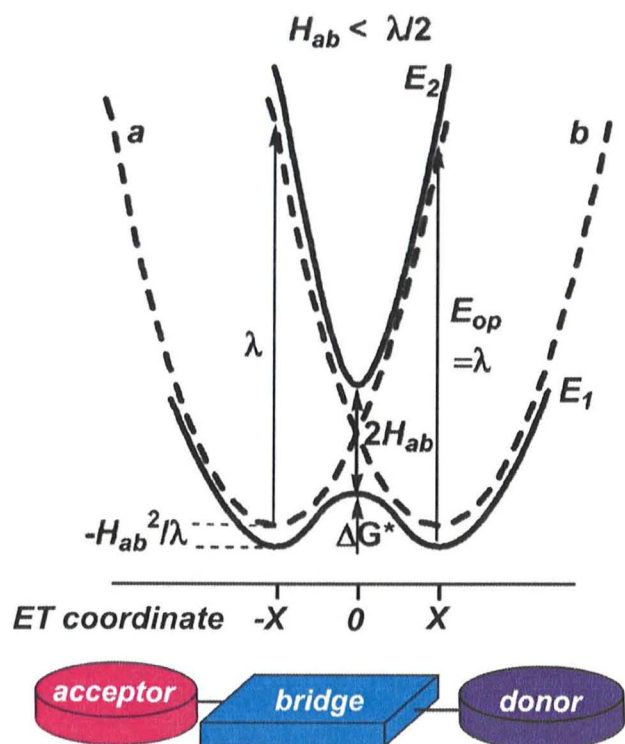


Fig. 2. Energy hypersurface of a mixed-valent compound of Class II (figure adapted from Ref. [40] with permission).

symmetrical stretch, i.e. the site with higher oxidation state is expanded from its equilibrium structure while the one with the lower oxidation state is contracted. For less symmetric systems the prerequisite structural changes involve more than just one such mode and are a more complex combination of several of them [13–16].

For MV compounds of Class II electronic coupling between the two redox sites leads to an avoided crossing of the individual diabatic hypersurfaces, which are usually assumed to have the hyperbolic shape of harmonic vibrations. This leads to a double minimum ground state, where the two minima at ET values of $+X$ and $-X$ are symmetrically displaced from an ET coordinate value of 0. This latter value denotes a fully symmetrical structure including the local redox sites and the bridge. The vertical displacement of the antibonding state with respect to the bonding one at the ET coordinate value of 0 is twice the electronic coupling matrix element H_{AB} . Intramolecular electron transfer can then occur in two ways: (i) as a thermally activated process where the system moves from one minimum of the lower adiabatic hypersurface to the other minimum by crossing the barrier separating them, and (ii) as a vertical electronic transition originating from one minimum of the lower adiabatic ground state to the Franck-Condon excited, antibonding state. From there, the excited electron may relax to the other ground state minimum. The latter event results in electron transfer from the former donor to the former acceptor site with a concomitant change of valencies. The underlying electronic transition is therefore dubbed as the “intervalence charge transfer” or IVCT band. Not surprisingly, much useful information on the electronic coupling matrix element H_{AB} can be gleaned from this band. The excitation energy equals the total reorganization energy λ which summarizes contributions from the reorganization of the internal structural parameters λ_{in} and of the reorganization of the solvent shell surrounding the individual redox sites λ_{out} . Both

need to adjust to the changing electron distributions upon intramolecular electron transfer.

MV systems of Robin and Day Class III have the minima of their ground and excited MV states at the ET coordinate value of 0 (see Fig. 3). This means that both states have fully symmetrical structures and symmetrical electron and spin density distributions. The electronic transition between these states is therefore called a charge resonance band, a term that was originally introduced to denote electronic bands that were observed for radical cations or anions of aromatic compounds in the presence of the neutral arene [17–19]. This transition does not induce a shift of charge density from one of the individual redox sites to the other but resembles more a transition within a delocalized chromophore.

How may one now obtain experimental information on the electronic coupling strength H_{AB} and on the rate of intramolecular ET? Following a rule of thumb, electronic coupling within a MV system should lead to a splitting of half wave potentials for the consecutive oxidations or reductions of the individual redox sites, and that splitting should increase as the electronic coupling increases. The rationale behind is that electronic coupling is expected to thermodynamically stabilize the MV state with respect to the bordering isoivalent states. This stabilization is measured by the comproportionation constant K_{comp} as given in Eq. (1). The relation between K_{comp} , the total free enthalpy ΔG of the comproportionation reaction, and the splitting of half wave potentials, $\Delta E_{1/2}$, is given by Eq. (2). One has to bear in mind, however, that $\Delta E_{1/2}$ mirrors the free enthalpy changes upon the individual consecutive one electron transfer steps just as a redox potential mirrors the difference in total free enthalpies of the oxidized and the reduced redox congeners. It is thus subject to several contributions besides the “resonance” term ΔG_{res} which corresponds to the electronic coupling (see Eq. (3)) [4,20–22]. First of all one has to consider electrostatic interactions ΔG_e . In the simplest case, that is, starting from a neutral compound, the MV species is a singly charged radical cation or

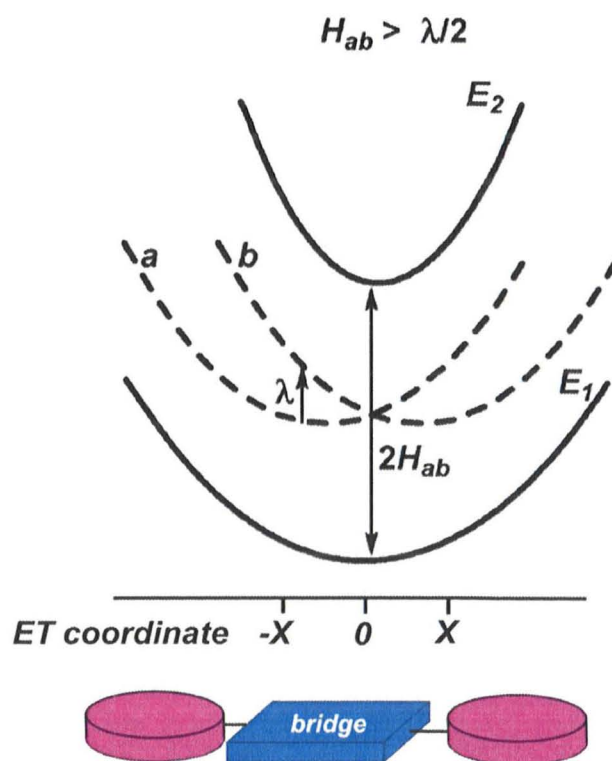
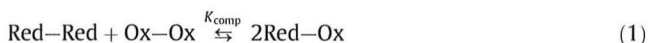


Fig. 3. Energy hypersurface of a mixed-valent compound of Class III (figure adapted from Ref. [40] with permission).

anion, respectively. Removal (or addition) of another unit charge upon the second one electron transfer process thus generates a doubly charged system with one charge at each of the local redox sites. This second process then suffers a Coulomb penalty as one more charge is extracted from (or added to) an already positively (negatively) charged system. This effect alone by itself will lead to a splitting of half wave potentials if the spatial separation between the two redox sites is not so large that the one is electrically insulated from the other. Another contributor to the overall ΔG is the inductive term ΔG_i . This term essentially accounts for the fact that electron transfer at one redox active subunit affects its bonding to the bridge. This effect is then in turn transmitted through the bridge to the other redox active subunit, thus changing the local electron density at this site and hence its intrinsic redox potential. Further terms are the magnetic exchange term ΔG_{ex} and the statistical term ΔG_s . The latter accounts for the fact that a system with two identical, independent redox sites will display a potential separation of $2 \ln 2RT/F = 36 \text{ mV}$ at $T = 298 \text{ K}$ between the individual redox processes [23]. What follows from this discussion is that the resonance term ΔG_{res} is only one contributor amongst several. Moreover, ΔG_{res} is usually considerably smaller than the Coulombic term ΔG_e , which often dominates the experimentally observed ΔG and $\Delta E_{1/2}$ values.

It has been shown that Coulombic interactions between adjacent redox sites do not only depend on the system itself but, to a large part, also on the experimental conditions of the electrochemical experiment such as the solvent and the supporting electrolyte [24–26]. Two examples may illustrate this point. The first involves the stepwise oxidation of the bis(fulvene) dinickel complex **1** of Chart 2. Varying the anion of the supporting electrolyte from Cl to the very weakly nucleophilic $[\text{B}(\text{C}_6\text{F}_5)_4]^-$ increases $\Delta E_{1/2}$ from 273 to 744 mV and K_{comp} by 7 orders of magnitude. These changes mirror the different degrees of electrostatic shielding of the two redox sites by their varying association with the counter ion of the supporting electrolyte [26].



$$K_{comp} = \frac{[\text{Red-Ox}]^2}{[\text{Red-Red}][\text{Ox-Ox}]} \exp\left\{\frac{(nF\Delta E_{1/2})}{(RT)}\right\} \quad (2)$$

$$\Delta G = \Delta G_e + \Delta G_i + \Delta G_{ex} + \Delta G_s + \Delta G_{res} \quad (3)$$

The second example is about the stepwise dithiolene based reductions of the nickel complex $(\text{Fc}_2\text{C}_2\text{S}_2)_2\text{Ni}$, **2** of Chart 2. Here, the splitting between individual reduction potentials strongly depends on the solvent and the cation of the supporting electrolyte. Thus, replacing the bulky, weakly associating NBu_4^+ cation of the $\text{NBu}_4^+[\text{B}(\text{C}_6\text{H}_3(\text{CF}_3)_2)_4]^-$ salt by Na^+ in CH_2Cl_2 diminishes $\Delta E_{1/2}$ from 770 mV, i.e. a value that one would safely take as indicating fully delocalized Class III behaviour of the MV radical anion, to the statistical limit of 40 mV that one would expect in the absence of any electronic coupling [26]. These examples show, how experimental $\Delta E_{1/2}$ values may be governed by electrostatic interactions. This renders $\Delta E_{1/2}$ a rather qualitative indicator for electronic coupling in MV systems, even when data on closely related sets of compounds obtained under closely similar conditions of solvent, supporting electrolyte, analyte concentration and temperature are compared, and better measures for this quantity are warranted. Albeit there are several examples where the electronic coupling H_{AB} and $\Delta E_{1/2}$ go in parallel [9,27–30], there are also some where no such correlation exists [31]. One such example will be detailed in a later section of this account.

On discussing the potential hypersurfaces for ET reactions we have already pointed out that intramolecular ET in MV systems of Class II can be induced by irradiation into the corresponding IVCT band. As a matter of fact, this band offers perhaps the most straightforward access to the electron coupling matrix element H_{AB} . For moderately coupled mixed valent systems of Class II, H_{AB} can be calculated from Eq. (4) following the theoretical framework of Hush, i.e. only one excited state is taken into account and all potential wells are assumed to be harmonic [32,33]. In Eq. (4), ν_{max} , $\Delta\nu$, ϵ_{max} and r_{AB} denote the energy (in cm^{-1}) at the band maximum of the IVCT transition, the band width at half height (in cm^{-1}), the molar extinction coefficient at the band maximum in $\text{l mol}^{-1} \text{cm}^{-1}$ and the charge transfer distance, i.e. the spatial distance over which the electron moves during the IVCT excitation. The treatment of MV systems of Class III is even simpler: Here, H_{AB} is just half the energy at the maximum of the charge resonance band.

$$H_{AB} = 0.0205(\nu_{max} \cdot \Delta\nu \cdot \epsilon_{max})^{1/2} / r_{AB} \quad (4)$$

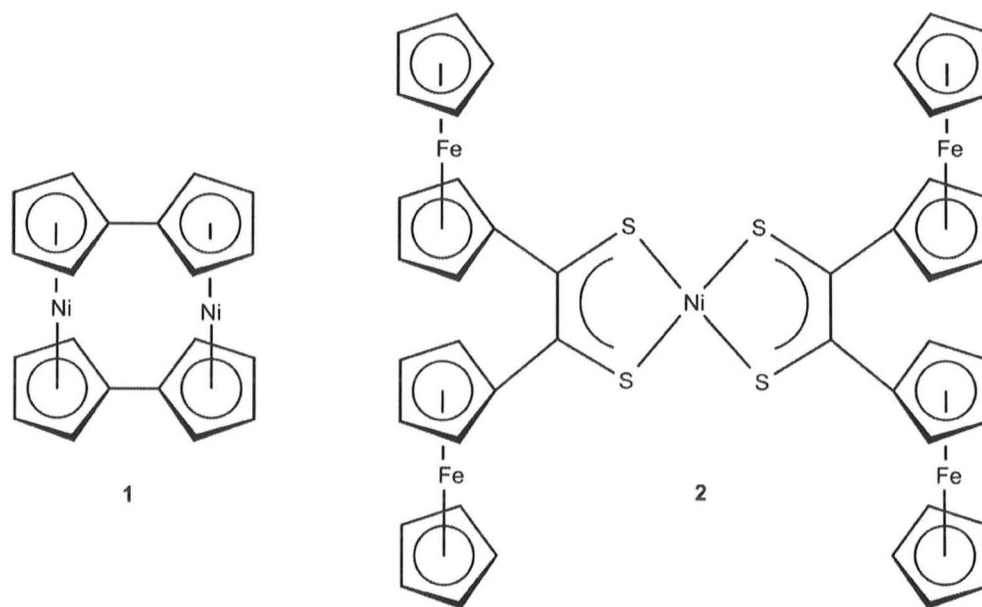


Chart 2.

The calculation of H_{AB} of Class II systems from IVCT band parameters is also not wholly without possible problems and pitfalls. One source of uncertainty pertains to the charge transfer distance r_{AB} . This parameter is often taken as the spatial separation between the centres of the bridged redox sites, which, in coordination compounds, are assumed to be the metal atoms. Such a procedure may, however, grossly overestimate r_{AB} with respect to the true electron transfer distance and, consequently, underestimate H_{AB} , particularly when the relevant “redox orbital” that is primarily involved in electron transfer delocalizes onto the bridge [34–38]. Unfortunately, the true electron transfer distance is notoriously difficult to come by experimentally, with electroabsorption (Stark) spectroscopy as about the only means. “All optical” and quantum chemical approaches to determine r_{AB} have also been reported but are anything but simple. In the case of quantum chemical approaches, the result strongly depends on the functional employed in the calculations [11,39–45].

Above that, the identification of the IVCT band as such is some times neither unambiguous nor trivial. An IVCT band usually occurs in the low energy part of the visible region or in the near infrared (NIR) and is “endemic” of the MV state but absent in the neighbouring isovalent ones. The specific appearance of a low energy electronic transition in the MV state is often taken as sufficient evidence for its assignment as such. Indeed, the specificity criterion usually distinguishes an IVCT band from d–d bands that may arise from abstracting an electron from the d manifold of a transition metal based redox site: the isovalent species resulting from electron transfer from the second of these sites also features such d–d bands. The same applies to ligand to metal charge transfer (LMCT) bands of metal oxidized forms or metal to ligand charge transfer (MLCT) bands of metal reduced forms since both types of transitions will occur in systems where either a single or both metal endgroups have undergone ET. It is, however, still possible, that singly oxidized radical cations of MV complexes display low energy metal to ligand charge transfer (MLCT) bands that correspond to the transfer of charge from the remaining reduced site to the now less electron rich bridging ligand or that radical anions of such systems display low energy ligand to metal charge transfer (LMCT) bands from the bridging ligand, which has gained electron density in the reduction process, to the remaining oxidized site. The probability of such transitions increases as the bridge becomes more and more involved in the ET process. In the case of more substantial or even dominating bridge contribution to the SOMO of the MV system, one may even observe low energy bands that resemble those expected for a bridge based radical cation or anion. Bands of such origin may also be specific to the MV state but should not be mistaken as IVCT transitions. We will discuss several such examples as we go along.

An elegant approach to finding out which class a certain MV system should be assigned to or to elucidating the rate at which intramolecular ET occurs is to furnish the redox active moieties or the bridge with spectroscopic tags which are indicative of the local charge or spin densities (which need not be the same) at these sites. Useful spectroscopic techniques include EPR spectroscopy, where information on the spin density distribution is encoded in the hyperfine splitting pattern to other nuclei bearing a nuclear spin, Moessbauer spectroscopy, where information on the valence state can be derived from the isotropic shift and the quadrupole splitting, or IR spectroscopy, where local vibrators whose force constants or band patterns are sensitive to the charge density on the redox active moiety or to the symmetry and the electron distribution within the bridge are required. Such role can be played by CO, NO, C≡N or C=C stretches of redox active moieties bearing carbonyl, nitrosyl, nitrile/isonitrile or alkylnyl tags. With respect to these spectroscopic techniques one should note that each of them is associated with its own inherent

time constant [46]. While the timescales of EPR (ca. 10^{-8} s) and of Moessbauer spectroscopy (ca. 10^{-9} s) are rather similar, vibrational motions occur at much faster rate of 10^{-11} to 10^{-12} s. IR spectroscopy is thus the method of choice for obtaining information about intrinsic (de)localization within a MV system [47]. One may envision a situation where a MV system appears to be delocalized by the EPR or Moessbauer techniques but localized on the faster IR timescale. Such behaviour has been observed and has been denoted as “time dependent valence trapping” (or detraping) [28,48]. It allows to bracket the time domain at which intramolecular ET occurs.

3. The vinyl ruthenium moiety: electron transfer properties and ligand non-innocence

Chart 3 schematically shows the types of vinyl ruthenium moieties that we have employed in our work as markers for intramolecular ET. The rather low and well accessible oxidation potentials, a stability of the various oxidized forms that allows for their (electro)chemical generation and spectroscopic characterization, the EPR activity of most of the aryl substituted vinyl complexes (except for those with acceptor substituents on the arene core) and the presence of one carbonyl ligand at each vinyl ruthenium site are factors that contribute to their great utility for this purpose. CO stretches of carbonyl ligands offer a highly convenient label for measuring the metal contribution to the relevant “redox orbital” and for obtaining information about the electronic equivalence or inequivalence of the individual vinyl ruthenium moieties and the ground state delocalization in the MV state of a complex comprising more than one such entity.

The synthesis of the vinyl ruthenium complexes of Chart 3 is simple and straightforward and involves the regio- and stereospecific insertion of a terminal alkyne into the Ru–H bond of a hydride complex $\text{RuClH}(\text{CO})(\text{PR}_3)_n$, where $n = 3$ for PAr_3 or 2 for bulky, strongly electron donating alkyl phosphines such as P^iPr_3 , $\text{P}(\text{cyclohexyl})_3$ or PPh^tBu_2 as the crucial step [49–54]. In this so called hydroruthenation any terminal alkyne will work unless it carries too bulky substituents to allow for formation of the primary alkyne associate preceding the insertion step as it is the case for $^t\text{BuC}\equiv\text{CH}$ or $(\text{CF}_3)_3\text{C}\equiv\text{CH}$ [55–58]. Upon alkyne insertion, the former hydride is transferred to the β carbon atom of the vinyl ligand and ends up at the same site as the ruthenium atom on C_2 . This means, that the Ru–CH=CHR unit inevitably has *trans* disposition of the R and the Ru “substituents” at the C=C double bond.

Starting from tris(triarylphosphine) hydride precursors, alkyne insertion usually generates a mixture of five- and six-coordinated complexes with three or only two phosphine ligands and an empty coordination site *trans* to the vinyl ligand. Binding of the third phosphine ligand is rather weak [59] such that this ligand can be removed by extraction into a suitable solvent or by precipitation of the five-coordinated complexes from hexanes/methanol mixtures. The five-coordinated 16 valence electron vinyl complexes thus obtained may accept a suitable donor ligand such as a pyridine, CO, an isonitrile, an amine, a nitrile and so on (Scheme 1). The easy substitution of the chloro ligand for another anionic mono- or bidentate ligand offers additional possibilities as to an *a posteriori* modification of the metal coordination sphere.

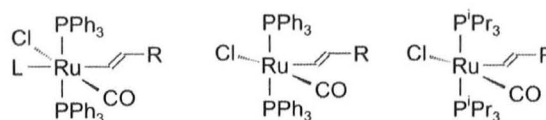
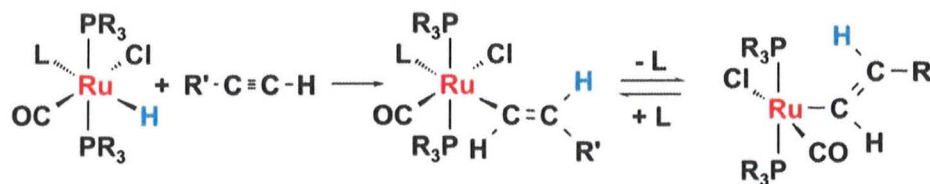


Chart 3.



Scheme 1.

The labile coordination of the third phosphine ligand in tris(triarylphosphine) vinyl ruthenium complexes is a consequence of the strong σ trans influence of the vinyl ligand and of steric crowding due to the meridional arrangement of three bulky phosphine ligands. It is thus more pronounced in complexes with bulky phosphines than in those with sterically less demanding ones like PMe_3 or PEt_3 . Complexes $\text{RuCl}(\text{2 pyrenylvinyl})(\text{CO})(\text{PPh}_3)_3$ ($d_{\text{Ru-P cis}}$ to vinyl range from 2.402(1) to 2.440(1) Å for the two independent molecules of the unit cell while $d_{\text{Ru-P trans}}$ to vinyl amounts to 2.585(1) or 2.564(1) Å) (Fig. 4) [60] and $\{\text{RuCl}(\text{CO})(\text{PMe}_3)_3\}_2(\mu\text{-CH=CH Aryl CH=CH})$, where the Ru-P bond trans to the vinyl ligand is by 4–12 pm longer than those *cis* to the vinyl ligand [61], may serve to illustrate this point. Five coordinated vinyl complexes assume a square pyramidal structure with the vinyl ligand, as the one with the largest σ trans influence of all ligands present, in the apical position [52]. The vinyl ruthenium entity is planar and parallel to the $\text{ClRu}(\text{CO})$ vector. In the solid state, the vinyl ligand is usually oriented towards the carbonyl ligand owing to secondary stabilizing π donor/ π acceptor interactions [62]. In aryl substituted vinyl complexes, the vinyl ruthenium moiety is more or less coplanar to the respective aryl substituent; torsional angles Ru-CH=CH-C(Aryl) typically range from about 5° to 20° . This already signals extended conjugation within the entire vinyl ruthenium moiety.

Mononuclear vinyl ruthenium complexes $\text{RuCl}(\text{CH=CHR})(\text{CO})(\text{PR}_3)_2\text{L}$ ($\text{R} = \text{Ph}$, $\text{L} = 4$ substituted pyridine, $\text{R} = \text{Pr}$, $\text{L} = \text{none}$) may now serve to introduce the reader to the basic properties of this class of compounds and to detail some of the points raised above. Electrochemical oxidation of these systems occurs as a chemically and electrochemically mostly reversible one electron process [58]. Exceptions are complexes with electron withdrawing substituents

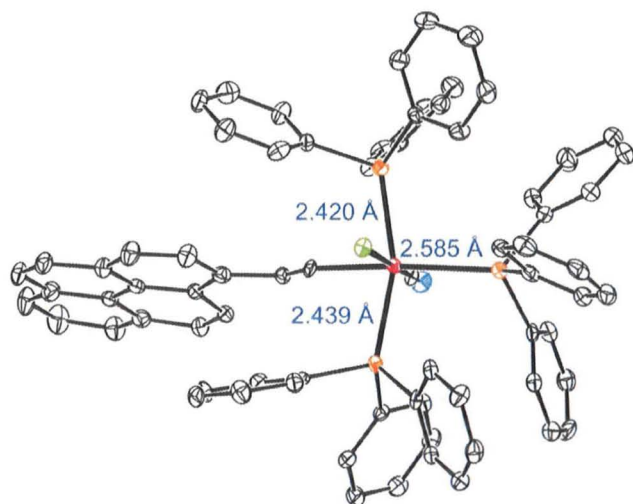


Fig. 4. Crystallographic structure of $\text{RuCl}(\text{CH=CH-2-pyrenyl})(\text{CO})(\text{PPh}_3)_3$ with Ru-P bond lengths (only one of the two crystallographically independent molecules is shown).

R' on the alkenyl ligand as in CH=CHCF_3 or $\text{CH=CH-C}_6\text{H}_4\text{NO}_2$ where partial decomposition of the associated radical cations already occurs on the voltammetric timescale. Conversion to 18 valence electron systems, e.g. by chloride replacement with carboxylates, generally helps to increase chemical reversibility of less reversible systems. Redox potentials strongly depend on the vinyl substituent as it is shown by the series of 4 substituted styryl complexes $\text{RuCl}(\text{CH=CH-C}_6\text{H}_4\text{X-4})(\text{CO})(\text{PMe}_3)_3$ [63] and $\text{RuCl}(\text{CH=CH-C}_6\text{H}_4\text{X-4})(\text{CO})(\text{P}^t\text{Pr}_3)_2$ [64], where shifts of 710 or 660 mV have been observed between $\text{X} = \text{NMe}_2$ and $\text{X} = \text{NO}_2$ as the two extremes. Complexes with donor substituted or more extended aryl substituents like $\text{CH=CH-C}_6\text{H}_4\text{NMe}_2$ or CH=CH-2-pyrenyl may also undergo a second reversible redox process at well accessible potentials. In these cases, the dioxidized dicationic species can also be generated and investigated (Fig. 5). For simple alkenyl and non donor substituted styryl complexes the second oxidation occurs as a chemically irreversible process at a significantly higher potential or, for acceptor substituted representatives, even outside the anodic limit of the $\text{NBu}_4\text{PF}_6/\text{CH}_2\text{Cl}_2$ supporting electrolyte.

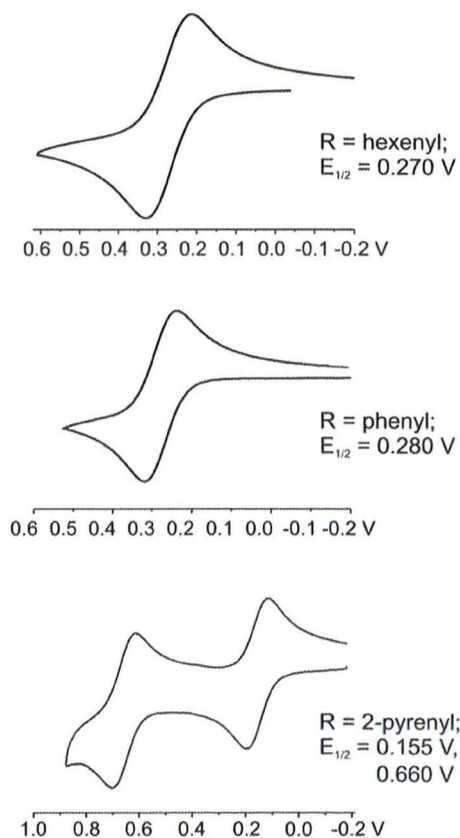


Fig. 5. Voltammograms ($\nu = 0.1$ V/s, 0.2 M NBu_4PF_6 in CH_2Cl_2 , rt) of complexes $\text{RuCl}(\text{CH=CH-R})(\text{CO})(\text{P}^t\text{Pr}_3)_2$.

The radical cations of aryl substituted complexes lacking a strong acceptor substituent are EPR active in fluid solution with isotropic g values of about 2.01–2.02. EPR spectra of P^iPr_3 complexes often display resolved hyperfine splittings to the ^{31}P and the $^{99/101}Ru$ nuclei. Set against the backdrop of the rapid spin lattice relaxation in “true” Ru^{III} paramagnetic species, necessitating low temperatures of about 100 K and frozen solvent matrices in order to detect their EPR signatures, the room temperature EPR activity of those systems comes as quite a surprise. There is another striking difference between the EPR spectra of more “conventional” organometallic Ru^{III} based and oxidized arylvinyl ruthenium complexes: the g values of the former differ more substantially from that of the free electron ($g_e = 2.0023$) and they usually exhibit rhombic or axial g tensors with anisotropies Δg in the range of 0.3 to >1.0 [65,66]. In contrast, oxidized vinyl ruthenium complexes $[RuCl(CH=CH\text{ Aryl})(CO)(PR_3)_2]^+$ (which were also Ru^{III} species if the oxidation was metal based) may display no g anisotropy at all or a significantly smaller g tensor splitting in frozen solution and in the solid state. Thus, Δg usually amounts to less than 0.03 in complexes bearing unsubstituted aryl substituents and scales with the Hammett parameter of the *para* substituent in 4 substituted styryl complexes [64]. Those observations designate oxidized alkenyl complexes as metal stabilized organic radicals. One might expect that ^{31}P and $^{99/101}Ru$ hyperfine coupling constants for oxidized vinyl ruthenium complexes provide an indicative handle for estimating the metal contribution to the SOMO. Unfortunately, there seem to be no such data for genuine paramagnetic Ru^{III} species to compare with. Based on these results, radical cations derived from vinyl ruthenium complexes are even more “organic” than those derived from oxidized 4 substituted phenylethynyl ruthenium complexes *trans* $[Cl(dppe)_2Ru\text{C}\equiv\text{C}\text{C}_6\text{H}_4\text{X}\text{4}]^+$ and $[Cp(dppe)Ru\text{C}\equiv\text{C}\text{C}_6\text{H}_4\text{X}\text{4}]^+$ [66,67], where the unsaturated organic ligand significantly contributes to the SOMO. It is therefore only fair to denote the alkenyl ligands in these complexes as “non innocent”, meaning that they actively participate in the redox process and generate considerable ambiguity about the metal oxidation state [68,69].

Additional experimental evidence for strong vinyl ligand participation to the SOMO comes from the observation of vibrationally structured bands in the low energy region of the visible or in the NIR for their radical cations (for an example see Fig. 6). Vibrational splittings are due to coupling of C=C stretching and C=CH bending modes to the electronic transition(s). Both is highly characteristic of unsaturated, conjugated organic radicals, but not of Ru^{III} paramagnetic species.

The synergistic nature of the metal carbonyl bond makes the energy of the CO stretch and its shift upon a redox process sensi-

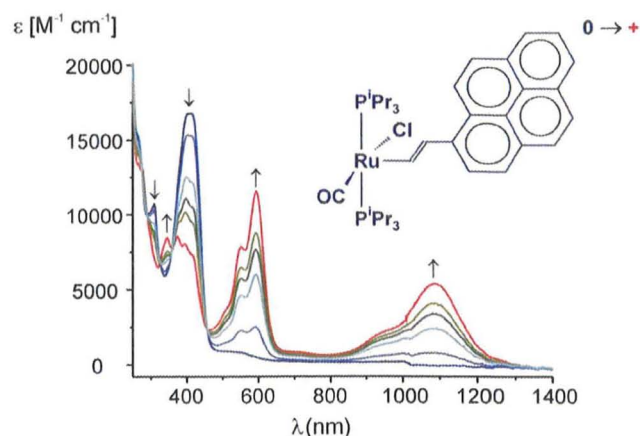


Fig. 6. Spectroscopic changes during electrochemical oxidation of $RuCl(CH=CH\text{-}2\text{-pyrenyl})(CO)(P^iPr_3)_2$ to its radical cation (0.2 M NBu_4PF_6 in 1,2- $C_2H_4Cl_2$, rt).

tive measures of the local electron density at the metal and its change upon addition or removal of an electron. A metal centred oxidation depletes the metal atom of d electron density and thus decreases backbonding to the π^* acceptor orbitals of the CO ligand. As a consequence, the CO force constant increases as lesser electron density flows into CO antibonding orbitals. The result is a sizeable blue shift of $\nu(CO)$ by about 120–150 cm^{-1} as it is observed, for example, in pairs of complexes $Ru(CO)_3(PR_3)_2^{0/+}$ [70].

We have prepared and investigated a series of substituted vinyl complexes that differ with respect to the spatial extension of the vinyl ligand's π system and observed a systematic decrease of the oxidation induced blue shift of $\nu(CO)$ with increasing conjugation length of that ligand (see Fig. 7) [60,64]. The CO band shift of complexes with even simple alkenyl ligands is only about half of that expected for a metal centred oxidation. We presently have no data that indicate to what extent the mutual *cis* disposition of the carbonyl and the vinyl ligands contributes to the small magnitude of this shift. We note, however, that quantum chemical calculations on somewhat simplified model systems (P^iPr_3 ligands modelled as PMe_3), while nicely reproducing our experimental observations including the qualitative magnitude of the CO band shift, also indicate a ca. 50% contribution of the hexenyl ligand to the HOMO of the reduced and to the SOMO of the oxidized form. Vinyl ligand contribution to these orbitals steadily increases as the butyl substituent is replaced by phenyl and by 2-pyrenyl. Control calculations of the exact model of $RuCl(CH=CHC_4H_9)(CO)$

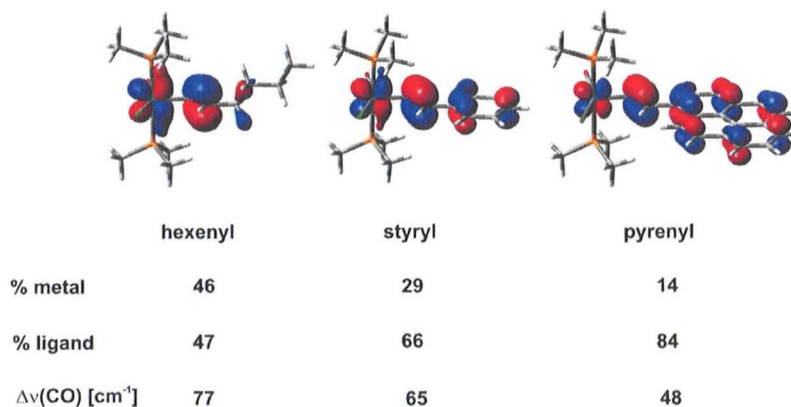


Fig. 7. Comparison of the experimental oxidation-induced shift of the $\nu(CO)$ band $\Delta\nu(CO)$ and of the computationally derived metal and vinyl ligand contribution to the HOMO along with graphical representation of the HOMOs.

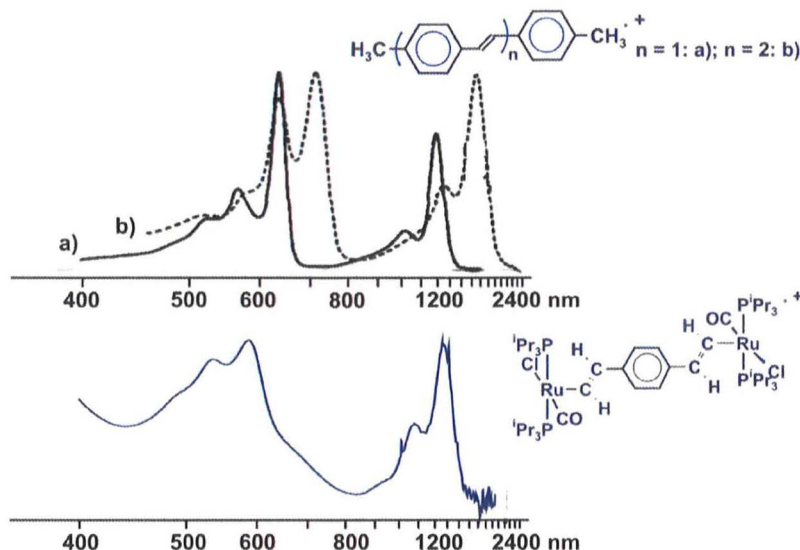


Fig. 8. Comparison of the Vis/NIR spectra of electrogenerated $[(\text{RuCl}(\text{CO})(\text{P}^i\text{Pr}_3)_2)(\mu\text{-CH=CH-C}_6\text{H}_4\text{-CH=CH-1,4})]^+$ and of those of 4,4'-dimethylstyrene and di(4-methylstyryl)benzene (adapted from Ref. [71] with permission).

$(\text{P}^i\text{Pr}_3)_2$ suggest that the simplifications introduced by substitution of the P^iPr_3 ligands by PMe_3 do not compromise the general conclusions drawn from the PMe_3 models [60,64].

The dominant organic character of arylvinyl substituted ruthenium complexes also explains, why the electronic spectrum of the radical cation of the divinyl phenylene bridged diruthenium complex $\{[\text{RuCl}(\text{CO})(\text{P}^i\text{Pr}_3)_2](\mu\text{-CH=CH-C}_6\text{H}_4\text{-CH=CH-1,4})\}^+$ closely resembles those of styryl type radical cations and, more specifically, that of oxidized distyrylbenzene [71,72]. The overall resemblance, as it is documented in Fig. 8, even pertains to the vibrational splitting constants which are virtually identical for both types of systems. From such comparison we can infer that the “ $\text{RuCl}(\text{CH=CH})(\text{CO})(\text{P}^i\text{Pr}_3)_2$ substituent” acts as nearly an as strong electron donor as the NMe_2 group while it simultaneously increases the conjugation length of the parent organic chromophore in basically the same manner as a coplanar phenyl ring. Vinyl ruthenium complexes are thus truly delocalized electroactive metal organic π systems.

4. Intramolecular electron transfer in vinyl-bridged diruthenium complexes

Forays into mononuclear vinyl ruthenium complexes have shown how electrochemistry and molecular spectroscopy in concert provide detailed information about the respective contributions of the metal atom and the ligand to the relevant “redox orbital”. We will now go one step further and address complexes with two vinyl ruthenium moieties or one vinyl ruthenium moiety and another redox active subunit. Here we will pose questions about charge and spin delocalization over the individual vinyl ruthenium subunits and the bridging ligand and the rate of intramolecular ET by making use of the various spectroscopic labels offered by the $\text{RuCl}(\text{CO})(\text{PR}_3)_2(\text{L})(\text{CH=CH})$ entities in very much the same manner as it was outlined in Section 2 of this account. In doing so, we will provide examples that we consider as being instructive to the reader. These examples will include linear systems, [2.2]paracyclophane derived systems exhibiting “3D type” delocalization and vinyl complexes having two different redox active subunits where only one of them is of vinyl ruthenium parentage.

4.1. Linear divinyl bridged diruthenium complexes

The first example of this class of compounds pertains to isomeric 1,3 and 1,4 divinylphenylene bridged diruthenium complexes $\{[\text{RuCl}(\text{CO})(\text{PR}_3)_2(\text{L})](\mu\text{-CH=CH-C}_6\text{H}_4\text{-CH=CH})\}$, **3** and **4**, with $\text{R} = \text{Ph}$, $\text{L} = 4 \times \text{C}_5\text{H}_4\text{N}$ ($\text{X} = \text{EtCOO}$, OMe , Me) or $\text{R} = ^i\text{Pr}$, $\text{L} = \text{none}$ as they are depicted in Chart 4 [73,74]. Liu and coworkers have reported similar studies on a series of divinylphenylene bridged dinuclear complexes $\{[\text{RuCl}(\text{CO})(\text{PMe}_3)_3](\mu\text{-CH=CH-ph}^{\text{R}}\text{-CH=CH})\}$ ($\text{ph}^{\text{R}} = \text{substituted phenylene unit}$), but only *para* isomers were investigated [61]. Every complex of Chart 4 is oxidized in two consecutive one electron waves. The splitting of half wave potentials, $\Delta E_{1/2}$, is very similar or even identical for the *para* and *meta* isomers. This is somewhat counterintuitive when taking the $\Delta E_{1/2}$ as a measure of electron delocalization in the corresponding singly oxidized MV system. Based on simple considerations of electronic interactions in *para* and *meta* disubstituted benzenes, much more substantial differences of $\Delta E_{1/2}$ would have been expected. Such behaviour was e.g. observed for 1,4 and 1,3 diethynylphenylene bridged diruthenium complexes *trans* $\{[\text{Cl}(\text{dppm})_2\text{Ru}]_2(\mu\text{-C}\equiv\text{C-C}_6\text{H}_4\text{-C}\equiv\text{C})\}$, where $\Delta E_{1/2}$ amounts to 300 mV for the *para* and to 190 mV for the *meta* isomers [75] despite a similar (though less strongly pronounced) non innocent character of the bis(ethynyl)phenylene bridging ligand [76–79]. EPR spectra of the PPh_3 derived radical cation complexes **4a-c**⁺ give only broadened isotropic signals with no resolved hyperfine splittings and thus provide no information about spin delocalization. For the P^iPr_3 derived systems *para* **3**⁺ and *meta* **3**⁺, however, hyperfine splittings to four equivalent ^{31}P and two equivalent $^{99/101}\text{Ru}$ nuclei were well resolved. This indicates a symmetrical spin distribution over both vinyl ruthenium subunits for the *meta* and the *para* isomer. The faster IR timescale of 10^{-12} s, however, reveals a difference: the radical cations of the PPh_3 derived complexes *para*-**4a-c** display only one single CO band indicating that the two $\text{RuCl}(\text{CO})(\text{PPh}_3)_2(4 \times \text{C}_5\text{H}_4\text{N})$ moieties are electronically equivalent. The five coordinated P^iPr_3 radical cation *para*-**3**⁺ is a less clear cut case in that two sets of overlapping $\text{Ru}(\text{CO})$ bands are observed, one with a single CO band and one consisting of two closely spaced $\text{Ru}(\text{CO})$ bands. The reason of such behaviour is still not entirely understood. A possible explanation is the coexistence of two isomers differing in the degree of electron

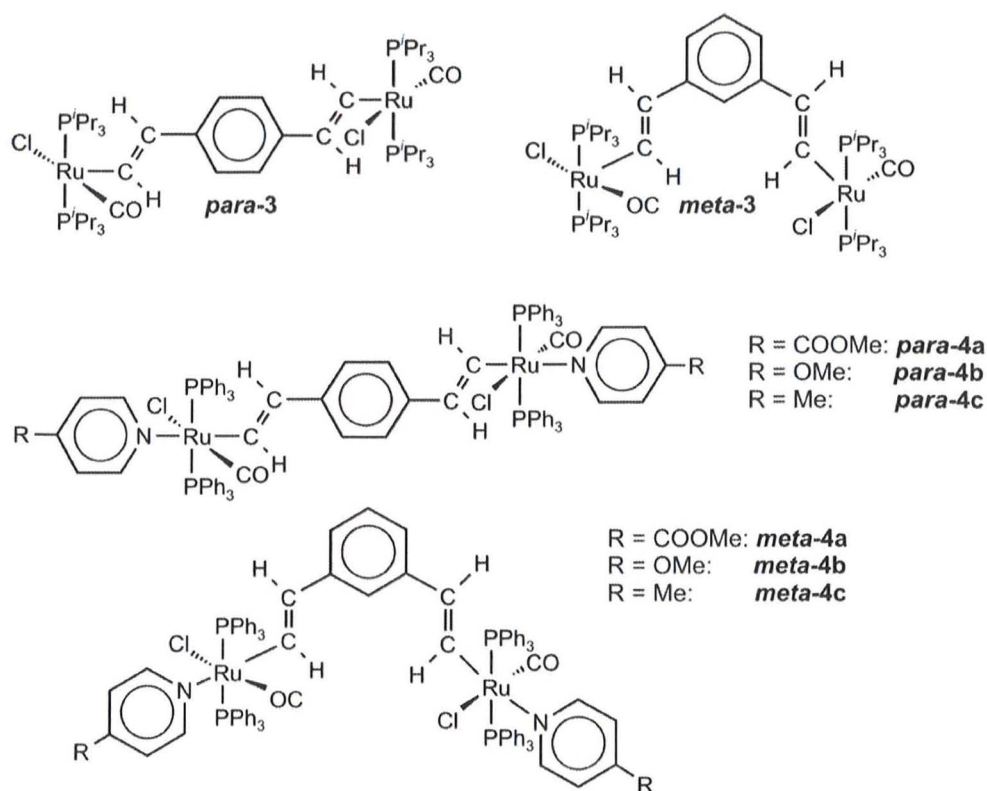


Chart 4. Divinylphenylene-bridged diruthenium complexes studied by us.

delocalization, possibly rotamers whose charge delocalization depends on the mutual orientations of the Ru(CO)Cl vectors [74].

All *meta* isomers, however, display a two band pattern with the CO band at the lower energy blue shifted with respect to the neutral complex and the higher energy band red shifted with respect to the doubly oxidized dication. This is the typical signature of MV systems of Class II with partially localized valencies and non symmetrical charge distributions over the two vinyl ruthenium subunits. Interestingly, the relative CO band shift as defined in Eq. (5) and illustrated in Fig. 9 yields a so called charge delocalization parameter $\Delta\rho$ which provides a quantitative measure of ground state charge delocalization [27,28]. By the definition of Eq. (5), $\Delta\rho$ may vary between the limits of 0 and 0.5. The lower limit of $\Delta\rho = 0$ characterizes MV systems of Class I with fully localized valencies. Here the lower and higher energy CO bands of the MV state are at the same position as in the neutral or in the diox

idized systems where both electroactive subunits are isovalent. In the other extreme, $\Delta\rho = 0.5$ denotes the limit of full charge delocalization where a single set of CO bands occurs at positions midway between those for the neutral and the dioxidized isovalent states. The relative CO band shifts for the three *meta* linked {RuCl(CO)(PPh₃)₂(4 X C₅H₄N)}₂(μ CH=CH C₆H₄ CH=CH 1,3) complexes yield $\Delta\rho$ values in the range of 25–32%, indicating that they are significantly coupled MV systems of Class II. For the radical cations of the *meta* isomers, intramolecular ET thus seems to occur at a time scale in between the EPR and IR time domains ($10^8 < k_{ET} < 10^{12}$ s⁻¹), while the radical cations of the *para* isomers are intrinsically delocalized MV radical cations of Class III.

$$\Delta\rho = \frac{\Delta\tilde{\nu}_{ox} - \Delta\tilde{\nu}_{red}}{2(\tilde{\nu}_{ox} - \tilde{\nu}_{red})} \quad (5)$$

Insertion of a further styryl unit into the bridge generates the distyrylethene bridged diruthenium complexes **5** and **6** of Chart 5. These may exist as *cis* or *trans* isomers, where the stereochemical discriminator pertains to the mutual disposition of the two styryl ruthenium subunits around the central C=C double bond. We were successful in preparing and structurally characterizing both isomers. As one might have expected, the central Ru-CH=CH-C₆H₄-CH=CH-C₆H₄-CH=CH-Ru unit of the *trans* isomer is fully planar, while in the *cis* isomer the phenyl planes are inclined by 38°. The *trans* isomer is oxidized in two consecutive one electron oxidations with a $\Delta E_{1/2}$ of just 35 mV ($K_{comp} = 4$) as shown by digital simulations of the experimental cyclic and square wave voltammograms. Such small redox splitting suggests an only modest electronic coupling between the styryl ruthenium subunits in the MV state. IR spectroscopy on the radical cation shows two separate CO bands, and both of them are appreciably shifted from their positions in the neutral and the dioxidized forms.

Electrocatalytic *cis* to *trans* isomerization at the radical cation stage **6**⁺ renders similar studies on the *cis* isomer impossible. We

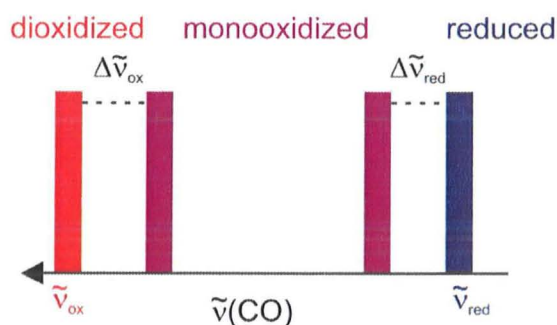


Fig. 9. Illustration of the band shifts utilized in determining the charge delocalization parameter.

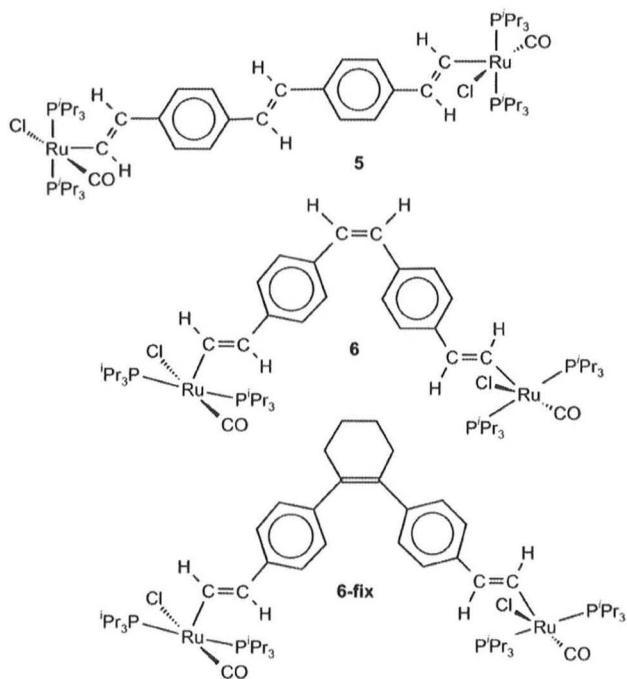


Chart 5. Distyrylbenzene-bridged diruthenium complexes studied by us.

therefore had to resort to a “cis fixated” analog **6-fix** where the central C=C double bond is incorporated into a cyclohexene ring (see Chart 5). This compound oxidizes in two consecutive one electron oxidation steps that are spaced by 63 mV ($K_{\text{comp}} = 12$) and thus by a larger amount than in the *trans* isomer. On stepwise oxidation we also observe a two band pattern for the radical cation with, however, significantly smaller relative CO band shifts than for the *trans* isomer. Data analysis yields $\Delta\rho$ values of 23% and 8% for the *trans* and the *cis* fixated isomers **5**⁺ and **6-fix**⁺. This is a case where $\Delta E_{1/2}$ and the “true” electronic coupling follow opposite trends. Coulomb contributions ΔG_e and the greater spatial proximity between the redox sites obviously override the resonance contribution ΔG_{res} to ΔG and K_{comp} .

4.2. Vinyl diruthenium complexes derived from cyclophanes

[n.n]Paracyclophanes are ideal testbeds for studying delocalization between stacked arene decks [80]. The groups of Neugebauer [81,82] and, more recently, Grampp and Lambert [83] have utilized EPR spectroscopy to probe for spin delocalization in radical cations derived from electron rich methoxy or bis(triarylamine) substituted [n.n]paracyclophanes. The decrease of electronic coupling with increasing extensions of the individual π decks and with increasing lengths of the alkyl straps were ascribed to the dilution of spin density on each of the conjoined, parallel displaced benzene rings and the decreased likeliness with which the system adopts conformations with small stacking distances.

We felt that the presence of the Ru(CO) units and the incremental CO band shifts upon stepwise oxidation would allow us to probe for *intrinsic* charge delocalization in such systems on the faster IR timescale. We thus prepared and investigated the pseudo para-(distyrylruthenium) [2.2]paracyclophane complex **8** of Chart 6 and the mononuclear and “half open” derivatives **7** and **9**. X ray structure analysis of **8** shows the expected features of this class of compounds such as a boatlike distortion of the arene decks with

the linked bridgehead carbon atoms as the bow and stern, a stacking distance of 3.065 Å between the best planes of the remaining four carbon atoms of each deck and near coplanarity of the ruthenium vinyl unit and the plane of the four non bridgehead carbon atoms of each deck. Complex **8** is oxidized in two consecutive one electron steps with $\Delta E_{1/2}$ of 215 mV. In its IR spectrum, radical cation **8**⁺ shows two well separated $\nu(\text{CO})$ bands. Again the low energy band is blue shifted with respect to the single CO band of the neutral. Further oxidation to the dication **8**²⁺ restores the one CO band pattern and reveals that the higher energy CO band of the radical cation is appreciably red shifted with respect to the carbonyl absorption of the dication. As discussed before, the relative CO band shifts of the radical cation provide a quantitative measure for ground state delocalization. The charge delocalization parameter $\Delta\rho$ thus obtained is 0.08. This essentially means that one of the Ru(CO) subunits bears less than 10% of the total positive charge on both Ru(CO) entities while the remaining >90% reside on the other one.

There is a general consensus that through space (i.e. π stacking) and through bond pathways (i.e. electron delocalization over the alkylene straps) are both relevant for electron delocalization in [n.n]paracyclophanes [30,83]. Several examples in the literature report on nonzero electronic couplings over simple alkyl connectors [84–88]. It is nevertheless hard to extract any quantitative information as to the relative contributions of the two complementary pathways from the literature data. In order to assess the relative contributions of the π stacking and σ bond pathways to the total delocalization we have prepared and investigated complex **9** of Chart 6. Complex **9** can be regarded as a half open orthocyclophane. The placement of an ethylene linker *para* to the vinyl ruthenium units and of a shorter methylene linker *meta* to them was intended to render both σ bond pathways as similar to complex **8** as possible and to prevent conformations with parallel displaced arene decks. Complex **9** also undergoes two consecutive reversible one electron oxidations which are separated by 105 mV. Stepwise oxidation inside a thin layer electrolysis cell first generates the radical cation and then the dication. In this case the low energy CO stretch of **9**⁺ appears at nearly the same energy as in **9** while the

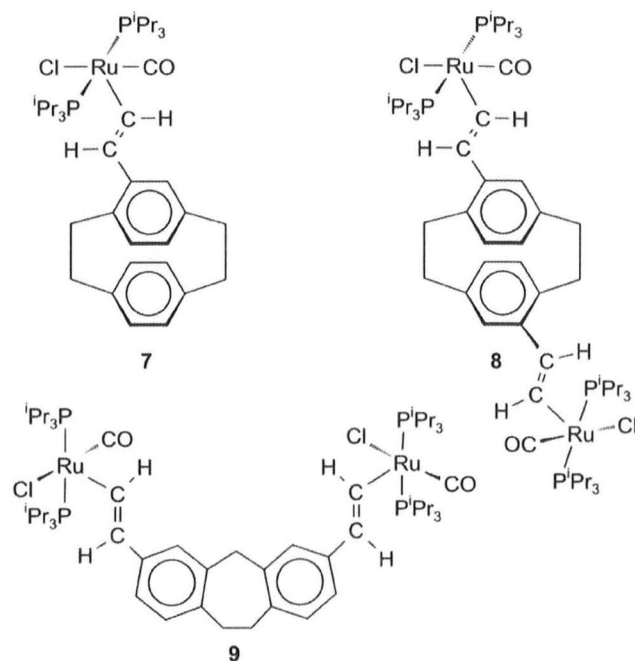


Chart 6. Cyclophane-derived vinyl ruthenium complexes studied by us.

band at higher energy is very close to the position of the CO band of 9^{2+} . From the IR criterion we can estimate the charge delocalization parameter of 9^{+} as about 0.01, which is substantially smaller than that in 8^{+} . Ground state delocalization in 8^{+} is a result of the combined effects of the through space and through bond pathways. In the half open cyclophane 9^{+} a parallel arrangement of the arene decks is conformationally unattainable. This particular constellation renders the through bond pathway the main contributor to the total electron delocalization in 9^{+} . From the comparison of the $\Delta\rho$ parameters of 8^{+} and 9^{+} we therefore conclude that π stacking constitutes the major pathway for overall electron delocalization in radical cations of [2.2]paracyclophanes while the through bond pathway contributes considerably less [89].

4.3. Mixed systems with only one vinyl ruthenium unit

The systems discussed in the previous sections were intended as illustrative examples of how vinyl ruthenium moieties can be employed to measure electron or spin delocalization in mixed valent systems incorporating two *identical* such units. In this final section we provide two examples of how they can be employed for measuring delocalization in MV systems containing two *different* redox active moieties where only one of them is of vinyl ruthenium parentage. The first example is the ferrocenyl vinyl complex $\text{Fc-CH=CH-RuCl}(\text{CO})(\text{P}^i\text{Pr}_3)_2$ (**10**, Chart 7) which is easily accessible from the hydorruthenation of ethynylferrocene. Complex **10** is oxidized in two one electron steps with a large $\Delta E_{1/2}$ of 715 mV which, however, this time is also due to the difference in intrinsic redox potentials of the two different redox active sub units. Structural comparison between the neutral and the chemically oxidized radical cation shows the familiar changes associated with the ferrocene to ferrocenium transformation such as a lengthening of all Fe–C bonds and a tilting of the cyclopentadienyl rings from a coplanar arrangement. There are, however, structural indications for the loss of charge from also the vinyl ruthenium part of this complex. Thus, the Ru–vinyl bond contracts by 4 pm while the Ru–C(CO) bond elongates by 3 pm [90].

Moessbauer and EPR spectra measured on powdered samples establish an only partial ferrocenium character of the radical cation and sizable charge and spin delocalization onto the vinyl ruthenium unit. Oxidation of **10** to 10^{+} diminishes the Moessbauer quadrupole splitting from 2.33 to 0.92 mm s^{-1} . While such behaviour is indicative of the loss of electron density from the ferrocenyl site, the observed quadrupole splitting of 10^{+} is appreciably larger than that for simple ferrocenium cations where it is usually lower than 0.15 mm s^{-1} and often below the resolution limit. The EPR signal of 10^{+} is already observed under liquid nitrogen cooling and displays the typical axial pattern of ferrocenium cations, but with an unusually small g anisotropy of less than 1. The parent ferrocenium ion and its simple ring substituted derivatives typically show $\Delta g > 2$ [91]. Both these anomalies are characteristic of ferrocenium type radical cations, where the ferrocenium moiety is embedded into an extended, π conjugated system or of partially delocalized biferrocenium radical cations. Hendrickson and others

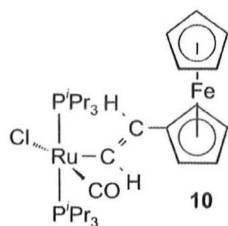
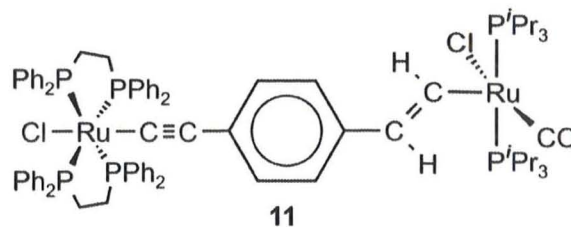


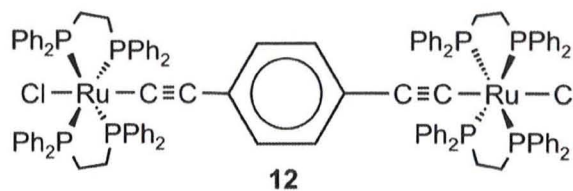
Chart 7. The ferrocenyl vinyl ruthenium complex studied by us.

[92] have established that Δg and the quadrupole splitting scale linearly with the fraction δ^+ of a unipositive charge on the ferrocene part of such structures. Taking their relations one arrives at a δ value of 0.8 for solid samples at liquid nitrogen temperature.

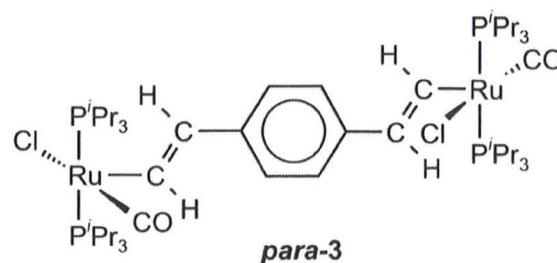
We can again nicely employ IR spectroscopy for monitoring the charge distribution in fluid solution. Here, the Ru(CO) band shifts



n =	0	1	2
$\tilde{\nu}(\text{C}\equiv\text{C}) =$	2065	2061, 1967	1891
$\tilde{\nu}(\text{C}\equiv\text{O}) =$	1910	1929	1977
$\tilde{\nu}_{\text{max}} =$		7460 cm^{-1}	
$E_{1/2}^{0/+} = -0.22 \text{ V}, E_{1/2}^{+/2+} = +0.14 \text{ V}$			



n =	0	1	2
$\tilde{\nu}(\text{C}\equiv\text{C}) =$	2071	2068, 1966	1918
$\tilde{\nu}_{\text{max}} =$		6553 cm^{-1}	
$E_{1/2}^{0/+} = -0.33 \text{ V}, E_{1/2}^{+/2+} = +0.01 \text{ V}$			



n =	0	1	2
$\tilde{\nu}(\text{C}\equiv\text{O}) =$	1910	1932	1991
$\tilde{\nu}_{\text{max}} =$		7970 cm^{-1}	
$E_{1/2}^{0/+} = -0.075 \text{ V}, E_{1/2}^{+/2+} = +0.175 \text{ V}$			

Chart 8. Spectroscopic data of the diethynylphenylene-bridged complex **12**, the divinylphenylene-bridged diruthenium complex *para-3* and the mixed alkynyl/vinyl phenylene-bridged complex **11** in their various oxidation states.

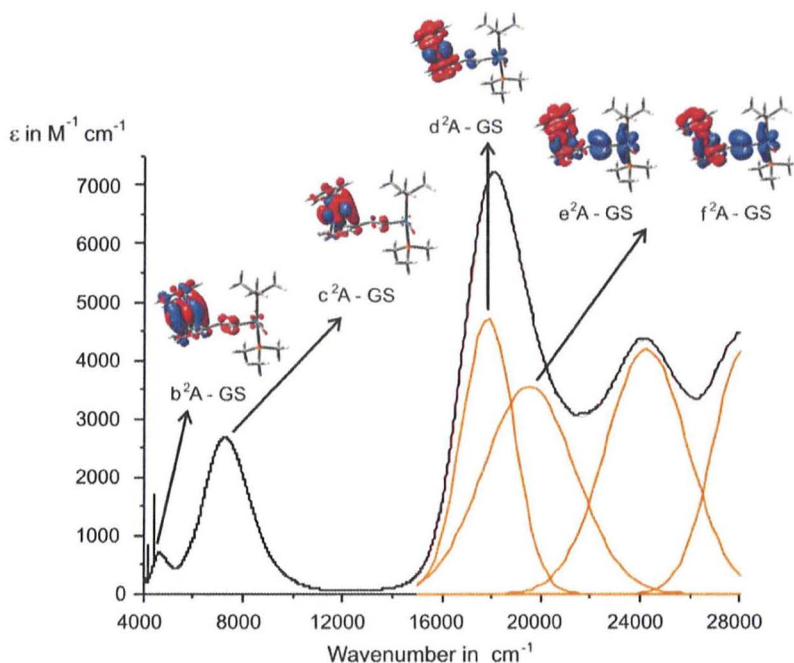


Fig. 10. Vis/NIR spectrum of radical cation 10^+ along with a deconvolution of the Vis bands and the charge density changes calculated by TD DFT. The plots show the charge shifts for each relevant excitation. Blue colour denotes diminishing electron densities and red colour denotes increasing electron densities.

by 24 cm^{-1} , which is 40% of the value in the related styryl complex $\text{RuCl}(\text{CH}=\text{CHPh})(\text{CO})(\text{P}^t\text{Pr}_3)_2$. By virtue of the $\nu(\text{CH})$ of the cyclopentadienyl ligands, complex 10 provides yet another charge sensitive IR label which is now attached to the ferrocene part of the structure. Here, $\nu(\text{CH})$ experiences a blue shift of 14 cm^{-1} , which is 60% of the value of the parent FcH/FcH^+ redox system [93]. Interestingly, solid samples show somewhat different values. Here the CO band shift reduces to 10 cm^{-1} while $\Delta\nu(\text{CH})$ increases to 24 cm^{-1} . The amount of charge on the $\text{Fc}^{\delta+}$ and the Ru $\text{CH}=\text{CH}^{(\delta)+}$ sites thus seems to depend on the environment. A close inspection of the crystallographic structure of 10^+PF_6^- offers a possible key to the reasons underlying this behaviour. The PF_6^- anions show no positional disorder and are associated to the cyclopentadienyl rings of the ferrocenyl substituents by a total of three $\text{CH}\cdots\text{F}$ hydrogen bonds that range from 2.37 to 2.52 Å. This ties the PF_6^- counterions to the $\text{Fc}^{\delta+}$ part of the structure and away from the Ru $\text{CH}=\text{CH}$ unit. Association through Coulombic forces may thus account for the higher charge concentration on the $\text{Fc}^{\delta+}$ site in the solid state and in polar environments as opposed to less polar solvents. Although similar counterion effects on charge delocalization are well documented for biferrocenium radical cations [94–101], the above hypothesis still calls for verification through radical cation salts of more or less coordinating anions than PF_6^- . Work along these lines is presently being pursued in our laboratories.

At this point we recall our statement that the identification of an IVCT band in MV systems as such may be anything but trivial. The mixed $[\text{Fc}\text{CH}=\text{CH}\{\text{Ru}\}]^+$ cation 10^+ offers a nice example of such notion. The electronic spectrum of 10^+ features several bands in the visible and in the NIR that grow in during the first oxidation [90]. Time dependent density functional (TD DFT) calculations have been performed in an attempt to identify the underlying electronic transitions. The results of that study are displayed in Fig. 10 along with the experimental absorption spectrum. The redistribution of electron density upon every relevant electronic transition is indicated by colour coding where the blue colour marks regions from which electron density is lost and the red one those which

gain electron density. The two low energy NIR bands which are the logical candidates of an IVCT type transition are calculated to involve the Fe based δ orbitals of the $\text{Fc}^{\delta+}$ subunit with very minor charge transfer to the $\text{CH}=\text{CH}$ Ru $^{(\delta)+}$ site. This is because the receptor orbital weakly interacts with the $\text{CH}=\text{CH}$ Ru “substituent” while the donor orbital does not. The next, rather intense band in the experimental spectrum is due to an overlap of two underlying transitions as is shown by TD DFT and by the comparison of experimental spectra in solvents of different polarity. The lower energy component is calculated to involve charge transfer within the $\text{Fc}^{\delta+}$ part of the molecule from the iron atom to the π^* orbitals of the Cp rings. The higher energy component is calculated to consist of two nearly degenerate transitions involving charge transfer from the vinyl ruthenium to mostly Cp based π^* orbitals of the ferrocene unit. This band is perhaps closest to an IVCT transition.

The final example involves mixed ethynyl/vinyl phenylene bridged diruthenium systems. Within the field of organometallic mixed valent systems, 1,4 diethynylphenylene bridged dinuclear complexes have gained particularly popularity. This is mainly due to the good propensity of the 1,4 diethynylphenylene linker to electronically couple the bridged metal sites. It has turned out, however, that while such kind of reasoning is fully appropriate for most metal complexes, this is not so in the diruthenium case. The reason is the same as for the divinylphenylene bridged counterparts: The HOMO of the reduced forms and the SOMO of the mixed valent radical cations of diruthenium complexes are not metal based but are mainly centred on the bridging ligand [76–79]. Few systems with two different metal endgroups have also appeared in the literature [102–105]. In these cases, the primary oxidation is more or less localized on just one metal ethynyl site due to a pronounced redox asymmetry resulting from a large difference in oxidation potentials between the individual metal ethynyl sites. The iron ruthenium complexes $\text{trans X}(\text{dppe})_2\text{Ru}\text{C}\equiv\text{C}\text{C}_6\text{H}_4\text{C}\equiv\text{C}\text{Fe}(\text{dppe})\text{Cp}^*$ (dppe = 1,2 bis(diphenylphosphanyl)ethane, Cp^* = $\eta^5\text{-C}_5\text{Me}_5$, $\text{X} = \text{Cl}$, $\text{C}=\text{CPh}$) are an exception in that their radical cations are appreciably coupled mixed valent systems of Class II [106]. The intrinsic redox potentials of the 1,4 diethynyl

phenylene bridged diruthenium complexes *trans* $\{X(dppe)_2Ru\}_2(\mu C\equiv C C_6H_4 C\equiv C)$ [107] and the 1,4 divinylphenylene bridged diruthenium complex $\{(P^tPr_3)_2(CO)ClRu\}_2(\mu CH=CH C_6H_4CH=CH)$ [74] are rather close. This prompted us to investigate the mixed 1 ethynyl 4 vinylphenylene bridged complex **11** which blends both these motifs into one single system (see Chart 8) [108].

The mere comparison of redox potentials already shows a profound mutual influence of the two sites. Replacing the powerful $Cl(dppe)_2Ru C\equiv C$ donor by the less potent $(P^tPr_3)_2(CO)ClRu CH=CH$ one shifts the first oxidation potential anodically by 110 mV with respect to the bis(ethynyl) phenylene bridged complex $\{[Cl(dppe)_2Ru]_2(\mu C\equiv C C_6H_4 C\equiv C 1,4)\}$ **12** [107] while the second oxidation occurs at less positive potential than that in the divinylphenylene bridged system *para-3*. From the comparison of the redox potentials one might guess that the first oxidation is more biased on the ethynylruthenium site. Again we resorted to the reporter qualities of the vinyl ruthenium moiety in order to measure electron delocalization in the mixed valent state.

The $C\equiv C$ and CO stretching frequencies for the neutral, the radical cations and the dioxidized dications of these species are collected in Chart 8. It turns out that the main $C\equiv C$ stretch of the radical cation of the “mixed” complex **11** at 1967 cm^{-1} is at virtually the same position as in the monooxidized bis(ethynyl)phenylene bridged system **12**⁺. Moreover, the absolute shift is half of that found in the trimethylsilyl protected or unprotected precursors *trans* $XRu(dppe)_2(C\equiv C C_6H_4 C\equiv CR)$ ($R = H, SiMe_3$). In addition, the position of the CO band matches that in the radical cation of the symmetrical divinylphenylene bridged system *para-3*. From this we conclude that the radical cation **11**⁺ is fully delocalized despite the unlike $\{Ru\} C_2H_n$ endgroups.

Moreover, the NIR band of **11**⁺ is positioned midway between those of its symmetrical counterparts *para-3*⁺ and **12**⁺. The same holds for the EPR signatures. As for the divinylphenylene bridged radical cation *para-3*⁺, the spectrum is isotropic in fluid or frozen solution and in the solid, but the isotropic g value is in between those of *para-3*⁺ and **12**⁺. In summary, the mixed ethynyl/vinyl system is an example of a completely delocalized metal organic MV system with two redox active subunits of different parentage. This is despite the intrinsically different oxidation potentials of its two constituents.

5. Conclusions

The present account summarizes our work devoted to utilizing vinyl ruthenium moieties for monitoring charge and spin delocalization within the vinyl ruthenium moiety itself and in MV systems containing two such units. Our studies on mononuclear vinyl ruthenium complexes have shown that they resemble electron rich organic phenylene vinylenes with respect to their redox properties and do not display metal based oxidations. The vinyl ruthenium functionality is easily integrated into organic π systems and endows them with superior thermodynamic stabilities of even the higher oxidized forms (considering that the oxidations are mostly ligand centred) and further modification of their properties by substitution at the organic and the metal part of these structures is simple. Together with this stabilizing property, the availability of the characteristic and charge sensitive $Ru(CO)$ absorptions and their EPR activity make vinyl ruthenium complexes excellent markers for investigating intramolecular electron transfer processes. *Absolute* IR band shifts are indicative of metal contribution to the “redox orbital” while the number of CO bands and their *relative* shifts provide quantitative information on intrinsic ground state delocalization in their mixed valent states.

Our results on the 1,3 divinylphenylene bridged diruthenium complex $\{[(P^tPr_3)_2(CO)ClRu]_2(\mu 1,3 CH=CH C_6H_4 CH=CH)\}^+$ have

provided an example of how the availability of different spectroscopic labels that respond to different timescales helps to establish the rate of intramolecular electron transfer. Other examples have shown that the splitting of redox potentials, while providing quantitative information on the thermodynamic stability of a MV compound with respect to the bordering isovalent ones, does not necessarily scale with the electronic coupling. This is particularly so, when isomers differing with respect to the spatial distance between the redox sites and thus with respect to the strength of the electrostatic interactions are compared. We have also documented that low energy absorptions of MV compounds need not necessarily be IVCT bands and other origins have to be considered. This is important if misinterpretations based on Hush type analyses of such bands of unclear origin are to be avoided. In the light of our results, even the specific appearance of such a band in the MV state is no unequivocal proof for its IVCT character. One final comment pertains to the last set of systems with two different redox sites: even if the intrinsic redox potentials of the different constituents suggests a certain order of redox events, one can never be entirely sure and their MV states may still exhibit substantial charge and spin delocalization. It remains to be explored, how “organic” vinyl ruthenium complexes just are and how they perform as markers in systems of even increased complexity.

Acknowledgements

R.F. Winter wishes to acknowledge the contributions of those coworkers who were not mentioned as coauthors; their names can be found in the cited literature. He also expresses his gratitude to collaborators and colleagues who have helped with measurements, by providing samples of special alkynes or with their comments and helpful discussions. Great many thanks also go out to the various funding agencies who have financially supported the work presented here: Deutsche Forschungsgemeinschaft (DFG, Grants No. Wi1262/7 1 and 7 2), DAAD (joint PROCOPE project with Prof. Stéphane Rigaut, Université de Rennes), Bayerisch Französisches Hochschulzentrum (collaboration with Prof. Michael Knorr, Université de Besançon), and Alexander von Humboldt Stiftung (post doctoral support for Dr. Konrad Kowalski, University of Łódź). S. Zálaiš also wishes to acknowledge the Grant Agency of the Academy of Sciences of the Czech Republic and the Ministry of Education of the Czech Republic (Grant No. LD11086) for financial support (Grant KAN100400702).

References

- [1] P.J. Low, Dalton Trans. (2005) 2821.
- [2] C. Creutz, H. Taube, J. Am. Chem. Soc. 91 (1969) 3988.
- [3] J.E. Sutton, H. Taube, Inorg. Chem. 20 (1981) 3125.
- [4] D.E. Richardson, H. Taube, Coord. Chem. Rev. 60 (1984) 107.
- [5] W. Kaim, A. Klein, M. Glöckle, Acc. Chem. Res. 33 (2000) 755.
- [6] J.-P. Launay, Chem. Soc. Rev. 30 (2001) 386.
- [7] M.B. Robin, P. Day, Adv. Inorg. Chem. Radiochem. 10 (1967) 247.
- [8] B. Brunswig, C. Creutz, N. Sutin, Chem. Soc. Rev. 31 (2002) 168.
- [9] C. Lambert, G. Nöll, J. Am. Chem. Soc. 121 (1999) 8434.
- [10] S.F. Nelsen, Chem. Eur. J. 6 (2000) 581.
- [11] S.F. Nelsen, M.N. Weaver, J.P. Telo, J. Am. Chem. Soc. 129 (2007) 7036.
- [12] K.D. Demadis, E.-S. El-Samanody, G.M. Coia, T.J. Meyer, J. Am. Chem. Soc. 121 (1999) 535.
- [13] S.E. Bailey, J.I. Zink, S.F. Nelsen, J. Am. Chem. Soc. 125 (2003) 5939.
- [14] A.V. Szeghalmi, M. Erdmann, V. Engel, M. Schmitt, S. Amthor, V. Kriegisch, G. Nöll, R. Stahl, C. Lambert, D. Leusser, D. Stalke, M. Zabel, J. Popp, J. Am. Chem. Soc. 126 (2004) 7834.
- [15] R. Warratz, H. Aboulfadl, T. Bally, T. Tuzek, Chem. Eur. J. 15 (2009) 1604.
- [16] J.V. Lockhard, J.I. Zink, Y. Luo, M.N. Weaver, A.E. Konradsson, J.W. Fowble, S.F. Nelsen, J. Am. Chem. Soc. 128 (2006) 16524.
- [17] B. Badger, B. Brocklehurst, Trans. Faraday Soc. 66 (1970) 2939.
- [18] B. Badger, B. Brocklehurst, R.D. Russell, Chem. Phys. Lett. 1 (1967) 122.
- [19] D. Sun, S.V. Rosokha, J.K. Kochi, J. Am. Chem. Soc. 125 (2004) 1388.
- [20] J.E. Sutton, P.M. Sutton, H. Taube, Inorg. Chem. 18 (1979) 1017.
- [21] C.E.B. Evans, M.L. Naklicki, A.R. Rezvani, C.A. White, V.V. Kondratiev, R.J. Crutchley, J. Am. Chem. Soc. 120 (1998) 13096.

- [22] Y.-C. Lin, W.-T. Chen, J. Tai, D. Su, S.-Y. Huang, I. Lin, J.-L. Lin, M.M. Lee, M.F. Chiou, Y.-H. Liu, K.-S. Kwan, Y.-J. Chen, *Inorg. Chem.* 48 (2009) 1857.
- [23] J.B. Flanagan, S. Margel, A.J. Bard, F.C. Anson, *J. Am. Chem. Soc.* 100 (1978) 4248.
- [24] F. Barrière, N. Camire, W.E. Geiger, U.T. Mueller-Westerhoff, R. Sanders, *J. Am. Chem. Soc.* 124 (2002) 7262.
- [25] D.M. D'Alessandro, F.R. Keene, *Dalton Trans.* (2004) 3950.
- [26] F. Barrière, W.E. Geiger, *J. Am. Chem. Soc.* 128 (2006) 3980.
- [27] M.E. Stoll, S.R. Lovelace, W.E. Geiger, H. Schimanke, I. Hyla-Kryspin, R. Gleiter, *J. Am. Chem. Soc.* 121 (1999) 9343.
- [28] C.G. Atwood, W.E. Geiger, *J. Am. Chem. Soc.* 122 (2000) 5477.
- [29] T. Ito, T. Hamaguchi, H. Nagino, T. Yamaguchi, H. Kido, I.S. Zavarine, T. Richmond, J. Washington, C.P. Kubiak, *J. Am. Chem. Soc.* 121 (1999) 4625.
- [30] D.-L. Sun, S.V. Rosokha, S.V. Lindeman, J.K. Kochi, *J. Am. Chem. Soc.* 125 (2003) 15950.
- [31] M.-C. Chung, X. Gu, B.A. Etzenhouser, A.M. Spuches, P.T. Rye, S.K. Seetharaman, D.J. Rose, J. Zubietta, M.B. Sponsler, *Organometallics* 22 (2003) 3485.
- [32] N.S. Hush, *Prog. Inorg. Chem.* 8 (1967) 391.
- [33] K.Y. Wong, P.N. Schatz, *Prog. Inorg. Chem.* 28 (1981) 369.
- [34] D. Oh, M. Sano, S.G. Boxer, *J. Am. Chem. Soc.* 113 (1991) 6880.
- [35] G.U. Bublitz, W.M. Laidlaw, R.G. Denning, S.G. Boxer, *J. Am. Chem. Soc.* 120 (1998) 6068.
- [36] T.P. Treynor, S.G. Boxer, *J. Phys. Chem. A* 108 (2004) 1764.
- [37] P.H. Dinolfo, S.J. Lee, V. Coropceanu, J.-L. Brédas, J.T. Hupp, *Inorg. Chem.* 44 (2005) 5789.
- [38] K. Lancaster, S.A. Odom, S.C. Jones, S. Thayumanavan, S.R. Marder, J.-L. Brédas, V. Coropceanu, S. Barlow, *J. Am. Chem. Soc.* 131 (2009) 1717.
- [39] C.E.B. Evans, D. Ducharme, M.L. Naklicki, R.J. Crutchley, *Inorg. Chem.* 34 (1995) 1350.
- [40] S.F. Nelsen, A.E. Konradsson, M.N. Weaver, J.P. Telo, *J. Am. Chem. Soc.* 125 (2003) 12493.
- [41] R.C. Johnson, J.T. Hupp, *J. Am. Chem. Soc.* 123 (2001) 2053.
- [42] V. Coropceanu, M. Malagoli, J.M. André, J.L. Brédas, *J. Am. Chem. Soc.* 124 (2002) 10519.
- [43] A. Heckmann, C. Lambert, M. Goebel, R. Wortmann, *Angew. Chem., Int. Ed. Engl.* 43 (2004) 5851.
- [44] A. Heckmann, S. Amthor, C. Lambert, *Chem. Commun.* (2006) 2959.
- [45] A. Heckmann, C. Lambert, *J. Am. Chem. Soc.* 129 (2007) 5515.
- [46] A.B.P. Lever, Notes on time frames, *Comprehensive Organometallic Chemistry II*, vol. 2, Elsevier, Amsterdam, 2003, pp. 435–438.
- [47] R.R. Rocha, A.P. Shreeve, *Inorg. Chem.* 43 (2004) 2231.
- [48] C.G. Atwood, W.E. Geiger, A.L. Rheingold, *J. Am. Chem. Soc.* 115 (1993) 5310.
- [49] M.R. Torres, A. Vegas, A. Santos, *J. Organomet. Chem.* 309 (1986) 169.
- [50] A.F. Hill, in: D.E. Shriver, M.I. Bruce (Eds.), *Comprehensive Organometallic Chemistry II*, vol. 7, Pergamon, Oxford, 1995, pp. 399–411.
- [51] M.A. Esteruelas, H. Werner, *J. Organomet. Chem.* 303 (1986) 221.
- [52] H. Werner, U. Meyer, K. Peters, H.G. von Schnering, *Chem. Ber.* 122 (1989) 2089.
- [53] S.H. Liu, Y. Chen, K.L. Wan, T.B. Wen, Z. Zhou, M.F. Lo, I.D. Williams, G. Jia, *Organometallics* 21 (2002) 4984.
- [54] H. Xia, T.B. Wen, Q.Y. Hu, X. Wang, X. Chen, L.Y. Shek, I.D. Williams, K.S. Wong, G.K.L. Wong, G. Jia, *Organometallics* 24 (2005) 562.
- [55] J.T. Poulton, M.P. Sigalas, O. Eisenstein, K.G. Caulton, *Inorg. Chem.* 32 (1993) 5490.
- [56] A.V. Marchenko, H. Gérard, O. Eisenstein, K.G. Caulton, *N. J. Chem.* 25 (2001) 1382.
- [57] A.V. Marchenko, H. Gérard, O. Eisenstein, K.G. Caulton, *N. J. Chem.* 25 (2001) 1244.
- [58] F. Pevny, R.F. Winter, B. Sarkar, S. Zálaiš, *Dalton Trans.* (2010) 8000.
- [59] S.K. Seetharaman, M.-C. Chung, U. Englisch, K. Ruhlandt-Senge, M.B. Sponsler, *Inorg. Chem.* 46 (2007) 561.
- [60] J. Maurer, M. Linseis, B. Sarkar, B. Schwederski, M. Niemeyer, W. Kaim, S. Zálaiš, C. Anson, M. Zabel, R.F. Winter, *J. Am. Chem. Soc.* 130 (2008) 259.
- [61] X.H. Wu, S. Jin, J.H. Liang, Z. Yong, G.-A. Yu, S.H. Liu, *Organometallics* 28 (2009) 2450.
- [62] S.-H. Choi, I. Bytheway, Z. Lin, G. Jia, *Organometallics* 17 (1998) 3974.
- [63] X. Wu, T. Weng, S. Jin, J. Liang, R. Guo, G.-A. Yu, S.H. Liu, *J. Organomet. Chem.* 694 (2009) 1877.
- [64] S. Zálaiš, R.F. Winter, W. Kaim, *Coord. Chem. Rev.* 254 (2010) 1383.
- [65] R.F. Winter, F.M. Hornung, *Organometallics* 18 (1999) 4005.
- [66] N. Gauthier, N. Tchouar, F. Justaud, G. Argouarch, M.P. Cifuentes, L. Toupet, D. Touchard, J.-F. Halet, S. Rigaut, M.G. Humphrey, K. Costuas, F. Paul, *Organometallics* 28 (2009) 2253.
- [67] F. Paul, B.G. Ellis, M.I. Bruce, L. Toupet, T. Roisnel, K. Costuas, J.-F. Halet, C. Lapinte, *Organometallics* 25 (2006) 649.
- [68] C.K. Jørgensen, *Coord. Chem. Rev.* 1 (1966) 164.
- [69] M.D. Ward, J.A. McCleverty, *Dalton Trans.* (2002) 275.
- [70] S.J. Sherlock, D.C. Boyd, B. Moasser, W.L. Gladfelter, *Inorg. Chem.* 20 (1991) 3626.
- [71] M. Deussen, H. Bässler, *Chem. Phys.* 164 (1992) 247.
- [72] H. Bässler, M. Deußen, S. Heun, U. Lemmer, R.F. Mahrt, *Z. Phys. Chem.* 184 (1994) 233.
- [73] J. Maurer, Präparative, elektrochemische, spektroeletrochemische und quantenchemische Studien an Ruthenium-Vinylkomplexen: "Schuldiges" Verhalten in Organometallverbindungen, Logos Verlag Berlin GmbH, Berlin, 2007.
- [74] J. Maurer, B. Sarkar, B. Schwederski, W. Kaim, R.F. Winter, S. Zálaiš, *Organometallics* 25 (2006) 3701.
- [75] M.C.B. Colbert, J. Lewis, N.J. Long, P.R. Raithby, M. Younus, A.J.P. White, D.J. Williams, N.N. Payne, L. Yellowlees, D. Beljonne, N. Chawdhury, R.H. Friend, *Organometallics* 17 (1998) 3034.
- [76] M.A. Fox, R.L. Roberts, W.M. Khairul, F. Hartl, P.J. Low, *J. Organomet. Chem.* 692 (2007) 3277.
- [77] D.J. Armit, M.I. Bruce, M. Gaudio, N.N. Zaitseva, B.W. Skelton, A.H. White, B. Le Guennic, J.-F. Halet, M.A. Fox, R.L. Roberts, F. Hartl, P.J. Low, *Dalton Trans.* (2008) 6763.
- [78] M.A. Fox, J.D. Farmer, R.L. Roberts, M.G. Humphrey, P.J. Low, *Organometallics* 28 (2009) 5266.
- [79] C. Olivier, B. Kim, D. Touchard, S. Rigaut, *Organometallics* 27 (2008) 509.
- [80] S.F. Nelsen, A.E. Konradsson, J.P. Telo, *J. Am. Chem. Soc.* 127 (2005) 920.
- [81] A. Wartini, H.A. Staab, F.A. Neugebauer, *Eur. J. Org. Chem.* (1998) 1161.
- [82] A. Wartini, J. Valenzuela, H.A. Staab, F.A. Neugebauer, *Eur. J. Org. Chem.* (1998) 139.
- [83] D.R. Kattinig, B. Mladenova, G. Grampp, C. Kaiser, A. Heckmann, C. Lambert, *J. Phys. Chem. C* 113 (2009) 2983.
- [84] M. Carano, M. Careri, F. Cicogna, I. D'Ambra, J.L. Houben, G. Ingrosso, M. Marcaccio, F. Paolucci, C. Pinzino, S. Roffia, *Organometallics* 20 (2001) 3478.
- [85] M. Carano, F. Cicogna, I. D'Ambra, B. Gaddi, G. Ingrosso, M. Marcaccio, D. Paolucci, F. Paolucci, C. Pinzino, S. Roffia, *Organometallics* 21 (2002) 5583.
- [86] S.V. Lindemann, S.V. Rosokha, J.K. Kochi, *J. Am. Chem. Soc.* 124 (2002) 843.
- [87] S. Roué, C. Lapinte, T. Bataille, *Organometallics* 23 (2004) 2558.
- [88] C. Elschenbroich, J. Plackmeyer, M. Nowotny, A. Behrendt, K. Harms, J. Pebler, O. Burghaus, *Chem. Eur. J.* 11 (2005) 7427.
- [89] P. Mücke, M. Zabel, R. Edge, D. Collison, S. Clément, S. Zálaiš, R.F. Winter, *J. Organomet. Chem.* in press.
- [90] K. Kowalski, M. Linseis, R.F. Winter, M. Zabel, S. Zálaiš, H. Kelm, H.-J. Krüger, B. Sarkar, W. Kaim, *Organometallics* 28 (2009) 4196.
- [91] R. Prins, A.R. Korswagen, *J. Organomet. Chem.* 25 (1970) C74.
- [92] J.A. Kramer, D.N. Hendrickson, *Inorg. Chem.* 19 (1980) 3330.
- [93] H.P. Fritz, Infrared and raman spectral studies of π -complexes formed between metals and C_nH_n rings, in: F.G.A. Stone, R. West (Eds.), *Advances in Organometallic Chemistry*, vol. 1, Academic Press, New York, 1964, pp. 239–316.
- [94] D.N. Hendrickson, S.M. Oh, T.-Y. Dong, T. Kambara, M.J. Cohn, M.F. Moore, *Comm. Inorg. Chem.* 4 (1985) 329.
- [95] T.Y. Dong, C.-H. Huang, C.-K. Chang, H.-S. Hsieh, S.-M. Peng, G.-H. Lee, *Organometallics* 14 (1995) 1776.
- [96] R. Webb, P.M. Hagen, R.J. Wittebort, M. Sorai, D.N. Hendrickson, *Inorg. Chem.* 31 (1992) 1791.
- [97] T. Kambara, D.N. Hendrickson, T.-Y. Dong, M.J. Cohn, *J. Am. Chem. Soc.* 86 (1987) 2362.
- [98] M. Kai, M. Katada, H. Sano, *Chem. Lett.* 18 (1989) 1473.
- [99] T.-Y. Dong, D.N. Hendrickson, C.G. Pierpont, M.F. Moore, *J. Am. Chem. Soc.* 108 (1986) 963.
- [100] T.-Y. Dong, T. Kambara, D.N. Hendrickson, *J. Am. Chem. Soc.* 108 (1986) 4423.
- [101] T.-Y. Dong, T. Kambara, D.N. Hendrickson, *J. Am. Chem. Soc.* 108 (1986) 5857.
- [102] O. Lavastre, J. Plass, P. Bachmann, S. Guesmi, C. Moinet, P.H. Dixneuf, *Organometallics* 16 (1997) 184.
- [103] S.C.-F. Lam, V.W.-W. Yam, K.M.-C. Wong, E.C.-C. Cheng, N. Zhu, *Organometallics* 24 (2005) 4298.
- [104] K.M.-C. Wong, S.C.-F. Lam, C.-C. Ko, N. Zhu, V.W.-W. Yam, S. Roué, C. Lapinte, S. Fathallah, K. Costuas, S. Kahlal, J.-F. Halet, *Inorg. Chem.* 42 (2003) 7086.
- [105] H. Jiao, K. Costuas, J.A. Gladysz, J.-F. Halet, M. Guillemot, L. Toupet, F. Paul, C. Lapinte, *J. Am. Chem. Soc.* 125 (2003) 9511.
- [106] N. Gauthier, C. Olivier, S. Rigaut, D. Touchard, T. Roisnel, M.G. Humphrey, F. Paul, *Organometallics* 27 (2008) 1063.
- [107] A. Klein, O. Lavastre, J. Fiedler, *Organometallics* 25 (2006) 635.
- [108] F. Pevny, E. Di Piazza, L. Norel, M. Drescher, R.F. Winter, S. Rigaut, *Organometallics* 29 (2010) 5912.